

CALCULATIONS OF NEUTRON MULTIPLICITIES AND SPECTRA FOR DIFFERENT ACTINIDES

F.-J. HAMBSCH

EC-JRC-IRMM Retieseweg 111, B-2440 Geel, Belgium

E-mail: franz-josef.hambsch@cec.eu.int

Abstract:

Based on experimental fission yield and total kinetic energy data, new calculations of the prompt neutron multiplicity and spectra for $^{235}\text{U}(n,f)$ in the incident neutron energy range up to 50 MeV and for $^{252}\text{Cf}(\text{SF})$ have been performed.

For $^{252}\text{Cf}(\text{SF})$, the multi-modality of the fission process was taken into account. Additionally, a more realistic fission fragment residual temperature distribution as well as an anisotropy of the prompt neutron emission has been introduced leading to improved agreement with experimental results.

For $^{235}\text{U}(n,f)$ a new fission cross section calculation was necessary up to 50 MeV prior to being able to deduce the partial fission cross sections above the first fission chance and the corresponding cross-section ratios, important quantities entering the multiplicity and spectrum modeling.

1. Introduction

The neutron balance in present day reactor systems is a crucial quantity, which needs continuous attention. Refinements in modeling of the prompt neutron multiplicities and spectra are the key to improved predictions of criticality benchmark exercises. ^{235}U and ^{252}Cf are key isotopes, since the latter is an important prompt neutron spectrum standard and the former is the main isotope in today's fuel cycle. Hence, improved models to describe prompt neutron characteristics for the above mentioned isotopes are highly appreciated.

In this sense an improved version of the Los Alamos (LA) model [1] has been developed recently for the calculation of prompt fission neutron multiplicity (PFNM) and spectra (PFNS). Below the second chance fission threshold multi-modality of the fission process based on experimentally obtained fission mode parameters has been taken into account in case of $^{252}\text{Cf}(\text{SF})$. For $^{235}\text{U}(n,f)$ the "point by point" approach has been used, based on the available fission fragment mass yields, similar to Ref. [2]. Above the second chance fission threshold only the most probable fragmentation

approach is feasible, since for neighboring nuclei, in general, little information about the mass yield distribution is available.

2. $^{252}\text{Cf}(\text{SF})$

For spontaneous fission (SF) of ^{252}Cf much more effort than for other nuclei was devoted to the measurement and interpretation of the PFNS, because the spectrum shape is considered as a standard.

Hence, the PFNS could be evaluated only on the basis of the experimental data (free of any model). The standard evaluation was made by Mannhart [3]. The evaluation resulted in a chi-square per degree of freedom of nearly unity and indicated no real inconsistencies between the various experiments.

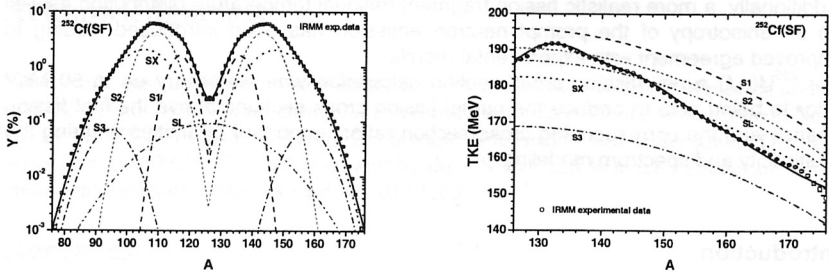


Figure 1. Multi-modal de-convoluted experimental data measured at IRMM. Shown is a superposition of 5 Gaussian distributions obtained from the analysis of the two-dimensional mass and TKE distribution. Mass yields and TKE as a function of fragment mass A are shown.

The multi-modal fission concept included into the LA model, has been successfully used in PFNS and PFNM calculations for several neutron induced reactions, see e.g. [4] and references therein. For $^{252}\text{Cf}(\text{SF})$ a similar approach has been followed [5]. The multi-modal parameters entering the PFNS model are determined on the basis of experimental data concerning the fission fragment (FF) total kinetic energy $\text{TKE}(A)$ and the FF mass distribution $Y(A)$ measured at IRMM (see Fig. 1).

In the present work the experimental data were fitted with five fission modes, four asymmetric modes named Standard I (S1), Standard II (S2), Standard III (S3) and Standard X (SX) and one symmetric mode named Super-long (SL). The existence of a weak contribution of the S3 mode had already been verified in case of neutron induced fission of ^{238}Np ($Z = 93$) [6] and ^{240}Pu ($Z = 94$) [7]. If it is a question of

compound nuclear charge whether new modes arise or not, in ^{252}Cf , with $Z = 98$, the contribution of S3 should be much higher. Hence, the need of five modes in case of $^{252}\text{Cf}(\text{sf})$ might be justified, following the trend of increasingly broader mass distribution with increasing Z , although no physical proof has been found so far. But from the theoretical calculations of the potential energy surface within the multimodal random neck-rupture model, even more modes have been predicted [8].

An important parameter entering the PFNM and PFNS calculations is the FF residual nuclear temperature distribution $P(T)$. Starting from the idea of Terrell [9] a new $P(T)$ distribution was used with a moderately broad high-temperature cutoff. This new $P(T)$ distribution is illustrated in Fig. 2 by the dashed line.

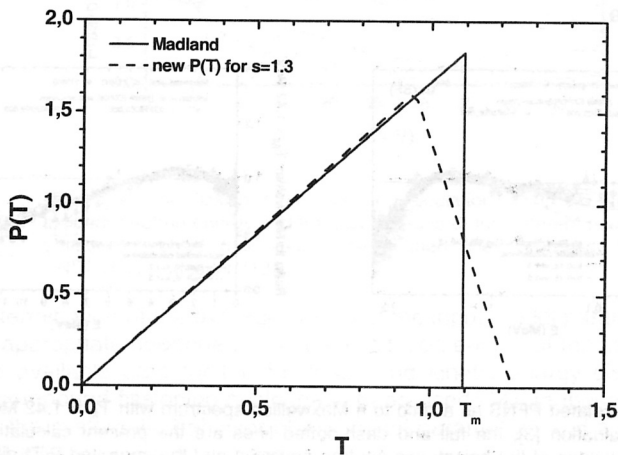


Figure 2. Improved residual temperature distribution following the idea of Terrell [9] and compared to the one used in Ref. [1] (full line).

Based on the improvements observed for $^{235}\text{U}(\text{n},\text{f})$ [4] also for $^{252}\text{Cf}(\text{SF})$ an anisotropy effect was introduced accounting for neutron evaporation during fragment acceleration which might be also possible [10] or neutron emission at scission, so-called scission neutrons. These neutrons can lead to a non-isotropic neutron

spectrum in the CMS. Presently, the search for scission neutrons is being performed, but so far with no definite conclusion. Our calculations can not distinguish between an anisotropy introduced by neutrons emitted during acceleration or due to scission neutrons. Nevertheless, the assumption of anisotropic neutron emission has improved the agreement between the calculated PFNS and experimental values (see Fig. 3).

It is evident from this figure that the inclusion of the anisotropy leads to a better agreement of the present calculation with Mannhart's evaluation. An increase of the PFNS in the low energy region (soft part of the spectrum) and a moderate increase at high fission-neutron energies (hard part of the spectrum) are visible. The increase of the PFNS in the low energy region is mainly due to the inclusion of the anisotropy of the neutron emission. At the high energy end, both contributions, anisotropy and $P(T)$ play a role.

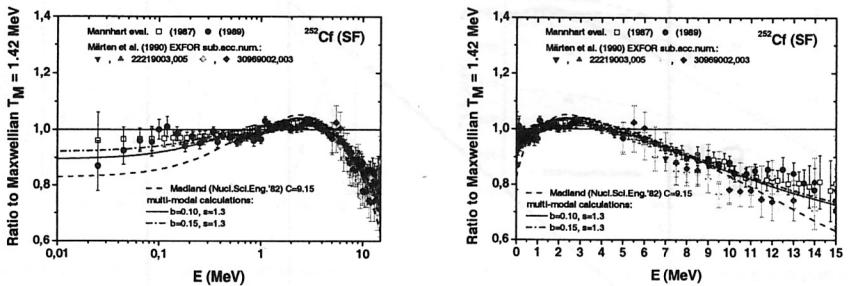


Figure 3. The calculated PFNS as a ratio to a Maxwellian spectrum with $T_M = 1.42$ MeV. Points are the Mannhart evaluation [3], the full and dash-dotted lines are the present calculation taking into account different values of the anisotropic neutron emission and the improved $P(T)$ distribution. The dashed line is the calculation of Madland [1].

3. $^{235}\text{U}(n,f)$

The improved LA model was also applied to the PFNM and PFNS calculations for $^{235}\text{U}(n,f)$ up to 50 MeV.

At higher incident neutron energies, where more than one fission chance is involved, the only way for a consistent calculation is to take into account the most probable

fragmentation for each residual compound nucleus (CN) [1,11,12] and to use average values for the input model parameters.

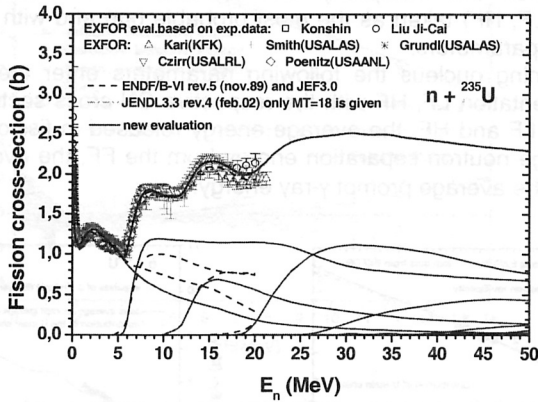


Figure 4. The fission cross section calculation up to 50 MeV incident neutron energy and the contributions of the different fission chances involved (full lines). The dashed lines represent the ENDF/B-VI evaluation [13].

For the determination of the average values of the input model parameters as well as their most appropriate dependence on the excitation energy of the fissioning nucleus, the scarce available data for the FF mass and kinetic energy distributions of the individual compound fissioning nuclei have been used [14]. In those cases, when no data exist, the systematic behavior of the model parameters and a simulation of the FF mass distribution have been used.

Another indispensable ingredient is the probability of each fission chance. This quantity can be obtained from the known multi-chance fission cross-sections [11]. The first three or four fission chance cross-sections are given in the evaluated nuclear data libraries only for a few major actinides.

In the present work the PFNM and PFNS calculations were made using the fission cross-section of the ^{235}U standard evaluation [13] (up to 20 MeV incident neutron energy) and the fission cross-section of a new ^{235}U cross-section calculation done up to 50 MeV incident neutron energy (see Fig. 4).

For higher fission chances, the calculation of the total PFNS and total PFNM requires to take into account the prompt neutron spectrum and multiplicity given by each compound fissioning nucleus (CN) involved in the studied reaction. For each CN undergoing fission the multiplicity and spectrum are calculated for a single fragmentation {LF, HF} taken as the most probable one and with average values of the input model parameters.

For each fissioning nucleus the following parameters enter the model, the most probable fragmentation LF, HF with the respective CN cross sections of the inverse process for the LF and HF, the average energy released in fission, the FF average TKE, the average neutron separation energy from the FF, the average level density parameter and the average prompt γ -ray energy.

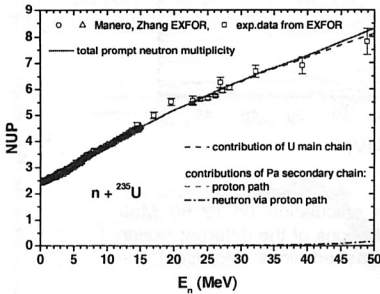


Figure 5. The calculated PFNM up to 50 MeV in comparison with experimental data from EXFOR [19].

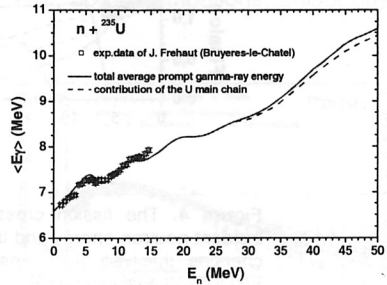


Figure 6. The calculated mean γ -ray energy up to 50 MeV in comparison with experimental data from EXFOR [19].

The PFNM and PFNS calculations for the $n + {}^{235}\text{U}$ reaction for incident neutron energies up to 50 MeV, were made with an improved version of the system of codes SPECTRUM [11]. The CN cross-sections for the inverse process were provided by the SCAT2 code [15] with the optical model potential of Becchetti-Greenless [16]. The CN formation cross-section of the fissioning nucleus was calculated using the coupled channel code ECIS95 [17] with our actinide deformed optical potential [18]. The PFNM calculation up to 50 MeV is given in Fig. 5 together with the experimental data taken from the EXFOR library [19]. As it can be seen, the total PFNM is obtained in good agreement with the experimental data in the entire range of studied incident neutron energies.

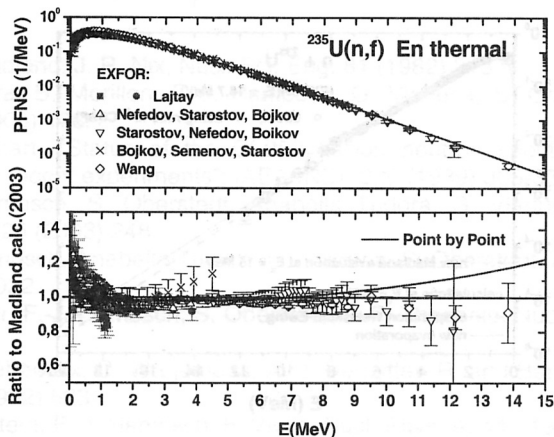


Figure 7. The PFNS at thermal energy in comparison with experimental data from EXFOR [15] and as a ratio to the most recent calculation by Madland [21].

Fig. 6 shows the total prompt γ -ray energy up to 50 MeV in comparison with the existing experimental data [20]. The excellent agreement with the experimental data is a supplementary test for the quality of the present PFNM and PFNS calculations.

The PFNS at thermal incident energy for the $^{235}\text{U}(n,f)$ reaction is shown in Fig. 7. For this nucleus the experimental data exhibit a large spread but the general agreement with the present calculations is again quite convincing. In the lower part of Fig. 7 the present PFNS calculation is given as a ratio to the recent calculation performed by D. Madland [21]. As it can be seen, the two calculations are rather close to each other and both in equal agreement with the widespread experimental data.

The PFNM and PFNS calculations at other incident neutron energies require to take into account the model parameter dependence [2,14] to the excitation energy of the fissioning compound nuclei taking part in the studied reaction.

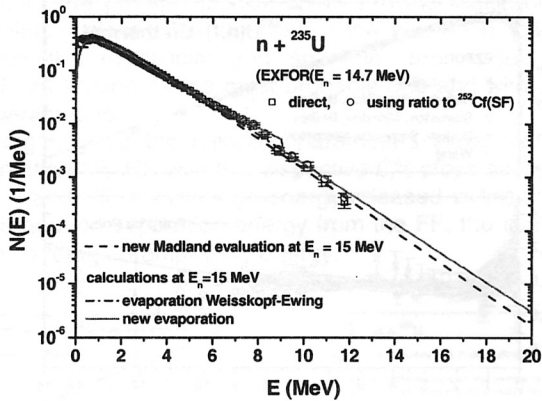


Figure 8. The PFNS at 15 MeV compared to experimental data from EXFOR [19] and the recent calculation of Madland [21].

The comparison of the present spectrum calculation with the existing experimental data [19] at incident energies, where multiple fission chances are involved, is given in Fig. 8, as an example, for 15 MeV. Also in this figure the new Madland calculations [21] are given with dashed lines. Above about a neutron energy of the emitted neutron of 6 MeV differences between the two calculations exist (more details can be found in Ref. [2]).

4. Conclusions

Including the multi-modality in the calculations of the PFNM and PFNS had already a positive effect on the agreement with experimental data [4]. Including a more realistic residual temperature distribution and an anisotropy of the prompt neutron emission gave even better agreement with the present evaluation data for $^{252}\text{Cf}(\text{SF})$. An extension of the cross section calculation was a necessary pre-requisite in case of the $^{235}\text{U}(n,f)$ reaction to be able to extend the PFNM and PFNS calculation up to 50 MeV incident neutron energy. Good agreement is observed both for the neutron spectra and prompt fission neutron multiplicity with available experimental data.

References

1. D. G. Madland, J. R. Nix, Nucl. Sci. Eng. 81 (1982) 213.
2. A. Tudora, B. Morillon, F.-J. Hamsch, G. Vladuca, S. Oberstedt, Nucl. Phys. A756 (2005) 176.
3. W. Mannhart, "Status of the Cf-252 fission neutron spectrum evaluation with regard to recent experiments"; IAEA-INDF 220 (1989) 305-336.
4. F.-J. Hamsch, S. Oberstedt, Anabella Tudora, G. Vladuca, I. Ruskov, Nucl. Phys. A726 (2003) 248.
5. F.-J. Hamsch, Anabella Tudora, G. Vladuca, S. Oberstedt, Annals Nucl. Eng. 32 (2005) 1032.
6. P. Siegler, F.-J. Hamsch, S. Oberstedt, J. P. Theobald, Nucl. Phys. A594 (1995) 45.
7. P. Schillebeeckx, C. Wagemans, A. J. Deruytter, R. and Barthelemy, Nucl. Phys. A545, (1992) 623.
8. S. Oberstedt, F.-J. Hamsch, F. Vivès, Nucl. Phys. A644 (1998) 289.
9. J. Terrell, Phys. Rev. 113 (1959) 527-541.
10. N. V. Kornilov, A. B. Kagalenko, F.-J. Hamsch, Phys. At. Nucl. 62 (1999) 173.
11. G. Vladuca, Anabella Tudora, Computer Phys. Communications 125 (2000) 221.
12. G. Vladuca, Anabella Tudora, Annals Nucl. Eng. 28 (2001) 419.
13. ENDF/B-VI rev.5 1997, file ZA92235, JEFF 3.0 file ZA092235, MF=3, MT=1, 2, 4, 16, 17, 37, 18, 19, 20, 21, 38.
14. A. Tudora, G. Vladuca, B. Morillon, Nucl. Phys. A740 (2004) 33.
15. O. Bersillon, SCAT2 optical model code OECD-NEA-DB-CPS package ID NEA0829/03, 1991.
16. Reference Input Parameter Library RIPL-1 - Segment 5 (Optical model parameters), recommended file IREF=100 (Becchetti-Greenless), 1998.
17. J. Raynal, ECIS95 code, private communication (1995) and J. Raynal, Notes of ECIS94, CEA-N-2772 (1994).
18. G. Vladuca, A. Tudora, M. Sin, Roum. J. Phys. 41, (1996) 515.
19. EXFOR nuclear data base (2001), nucleus 235U, quantity Prompt Nu, DE.
20. J. Frehaut, IAEA INDC(NDS)-220 (1989) 99.
21. D. G. Madland in NEA/WPEC-9 Fission Neutron Spectra of U-235 Report of the Working Party of Int. Evaluation Co-operation of the NEA Nucl. Sci. Committee (ODCE 2003), <http://t2.lanl.gov/data/fspect.html>.